

Analysis of a stochastic model for bacterial growth and the lognormality in the cell-size distribution

Ken Yamamoto and Jun-ichi Wakita
Department of Physics, Faculty of Science and Engineering,
Chuo University, Kasuga, Bunkyo, Tokyo 112-8551, Japan

This paper theoretically analyzes a phenomenological stochastic model for bacterial growth. This model comprises cell divisions and linear growth of cells, where growth rates and cell cycles are drawn from lognormal distributions. We derive that the cell size is expressed as a sum of independent lognormal variables. We show numerically that the quality of the lognormal approximation greatly depends on the distributions of the growth rate and cell cycle. Furthermore, we show that actual parameters of the growth rate and cell cycle take values which give good lognormal approximation, so the experimental cell-size distribution is in good agreement with a lognormal distribution.

I. INTRODUCTION

A. General overview

In the study of complex phenomena, we can extract statistically useful information from the size distribution of observed elements. Along with the power-law distribution[1, 2] which is closely associated with critical phenomena in statistical physics, the lognormal distribution [3] is found in a wide range of complex systems. [4, 5] It appears in natural phenomena such as fragment and particle sizes[6, 7], fluctuation of X-ray bursts[8], and genetic expression in bacteria[9], and in social phenomena such as population[10], citation of scientific papers[11], and proportional elections[12]. The commonness of the lognormal behavior is a clue to studying various complex systems from a unified viewpoint based on statistical physics.

A random variable X is said to follow a lognormal distribution $\ln \mathcal{N}(\mu, \sigma^2)$ if its logarithm $\ln X$ is normally distributed with mean μ and variance σ^2 . The probability density of $\ln \mathcal{N}(\mu, \sigma^2)$ is

$$f_{\mu, \sigma}(x) = \frac{1}{\sqrt{2\pi\sigma^2} x} \exp\left(-\frac{[\ln x - \mu]^2}{2\sigma^2}\right),$$

and the (upper) cumulative distribution function is

$$\begin{aligned} F_{\mu, \sigma}(x) &= \int_x^\infty f_{\mu, \sigma}(y) dy \\ &= \frac{1}{2} \left[1 - \operatorname{erf}\left(\frac{\ln x - \mu}{\sqrt{2}\sigma}\right) \right] = \frac{1}{2} \operatorname{erfc}\left(\frac{\ln x - \mu}{\sqrt{2}\sigma}\right), \end{aligned} \quad (1)$$

where $\operatorname{erf}(x) = (2/\sqrt{\pi}) \int_0^x \exp(-y^2) dy$ is the Gauss error function and $\operatorname{erfc}(x) = 1 - \operatorname{erf}(x)$ is the complementary error function[13]. The lognormal distribution is a heavy-tailed distribution; that is, the tail of $F_{\mu, \sigma}(x)$ decays slower than any exponential functions. Thus, a phenomenon obeying a lognormal distribution easily produces values far larger than the average. The average of the distribution $\ln \mathcal{N}(\mu, \sigma^2)$ is $\exp(\mu + \sigma^2/2)$, and the median is $\exp(\mu)$. The average is always larger than the

median, and this is a consequence of the heavy-tailed property of the lognormal distribution.[14]

The lognormal distribution is typically generated by a multiplicative stochastic process.[15] Consider a stochastic process X_1, X_2, \dots given by

$$X_{n+1} = M_n X_n,$$

where M_n is a positive random variable. If the growth rates M_1, M_2, \dots are independently and identically distributed, and satisfy that $E[\ln M_n] = \mu$ and $V[\ln M_n] = \sigma^2$ are finite, the central limit theorem yields that the distribution of $(\ln X_n - n\mu)/(\sqrt{n}\sigma)$ converges to the standard normal distribution (with zero mean and unit variance). Roughly speaking, the distribution of X_n for sufficiently large n is reasonably approximated by the lognormal distribution $\ln \mathcal{N}(n\mu, n\sigma^2)$. The lognormal parameters $n\mu$ and $n\sigma^2$ diverge as $n \rightarrow \infty$, so X_n itself does not have a stationary distribution exactly. Many kinds of systems have multiplicativity in some sense, so the lognormal distribution is a natural distribution for them[4].

We need to investigate carefully whether a probability distribution from actual data is truly lognormal or not, even if the lognormal fitting is visually successful. A lot of researchers have pointed out that a lognormal distribution can be confused with other probability distributions like power-law[16], normal[17], and stretched exponential[18] distributions. Furthermore, the multiplicative nature does not necessarily lead to a lognormal distribution. In fact, lognormal behavior can easily change into other distribution if additional rules are assigned to the multiplicative stochastic process. For instance, multiplicative processes with additive noise[19], reset event[20], and random stopping[21] produce power-law distributions. It is difficult to examine whether an experimental data set follows a genuine lognormal distribution or a lognormal-like distribution.

In this paper, we perform a theoretical analysis for a stochastic model of a bacterial cell size. Wakita *et al.*[22] have reported that the cell-size distribution of bacterial species *Bacillus (B.) subtilis* is well described by a lognormal distribution. They have also proposed a phenomenological stochastic model for the growth of bacterial cells,

and have confirmed that the numerical result reproduces the actual cell-size distribution quantitatively. In contrast to these results, we show in this paper that the cell-size distribution generated by this model is not a genuine lognormal distribution in reality. In order to elucidate the situation and problem we consider, let us give an outline of the experiment and model in the next subsection.

B. Experiment and modeling of bacterial cell size

As a background of the present paper, we concisely review the above-mentioned experimental study [22] regarding the cell-size distribution of *B. subtilis*, which is a rod-shaped bacteria of 0.5–1.0 μm in diameter and 2–5 μm in length. The morphology of a *B. subtilis* colony spreading on agar surface changes depending on nutrient and agar concentrations, and is classified into five types: diffusion-limited aggregation-like, Eden-like, concentric ring-like, homogeneously spreading disk-like, and dense branching morphology-like patterns. Relation between each pattern and the nutrient and agar concentrations is summarized in the form of a morphological diagram[23]. Bacterial colonies have been extensively investigated from the standpoint of physics, as a typical pattern-formation phenomenon that the different patterns appear by changing external conditions.[24]

According to the measurement of bacterial cells in homogeneously spreading disk-like colonies (formed in soft agar and rich nutrient), the cell size at the beginning of expanding phase follows the lognormal distribution $\ln\mathcal{N}(\ln 2.7, 0.24^2) = \ln\mathcal{N}(0.99, 0.24^2)$, whose median is $\exp(0.99) = 2.7 \mu\text{m}$. In addition, the cell length in lag phase has been reported to increase linearly with time up to the cell division. The cell cycle is represented by the lognormal distribution $\ln\mathcal{N}(\ln 22, 0.20^2) = \ln\mathcal{N}(3.1, 0.20^2)$ (the median is 22 min), and the growth rate also exhibits lognormal behavior with $\ln\mathcal{N}(\ln 0.078, 0.30^2) = \ln\mathcal{N}(-2.6, 0.30^2)$ (the median is 0.078 $\mu\text{m}/\text{min}$).

Based on these experimental results, a phenomenological model has been proposed. The procedure of this model is schematically shown in Fig. 1. The model starts with a single cell A of unit length, and assigns cell cycle τ_A and growth rate v_A drawn from lognormal distributions. Cell A grows linearly with time, i.e., the size of cell A at time $t < \tau_A$ becomes $1 + v_A t$. At $t = \tau_A$, cell A divides equally into two cells B and C. Growth rates v_B and v_C and cell cycles τ_B and τ_C are newly assigned. For simplicity, the growth rate and cell cycle of each cell are assumed to be independently distributed. The cells continue repeating linear growth and cell divisions in the same way. According to the numerical calculation[22], the cell-size distribution becomes stationary after a long time. By choosing realistic parameters in the lognormal distributions for the growth rate and cell cycle [namely, $\ln\mathcal{N}(3.1, 0.20^2)$ for cell cycles and $\ln\mathcal{N}(-2.6, 0.30^2)$ for growth rates], the resultant station-

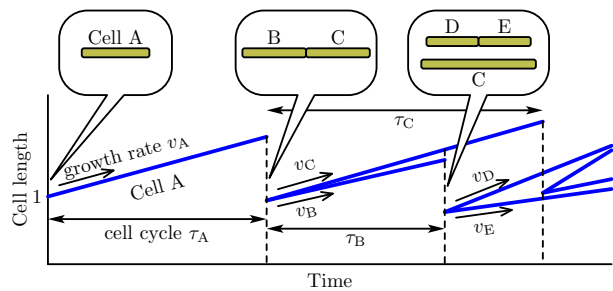


FIG. 1: Illustration of the model for growing bacterial cells. The initial cell A of unit length grows linearly by growth rate v_A , and it divides equally into two cells B and C at $t = \tau_A$. Cells B and C respectively grows linearly by rate v_B and v_C until the next cell division, and so forth. The arrangements of the cells at time $t = 0$ (initial state), $t = \tau_A$ (just after the first cell division), and $t = \tau_A + \tau_B$ (just after the second division) are schematically shown in the balloons.

ary distribution is described by $\ln\mathcal{N}(0.92, 0.28^2)$. This is in good agreement with the actual cell-size distribution $\ln\mathcal{N}(0.99, 0.24^2)$ of *B. subtilis*. Furthermore, it has been reported that the longnormal behavior in the numerical cell-size distribution disappears if the lognormal parameter σ of the growth rate or cell cycle is too small or too large.

We theoretically analyze this phenomenological model in the present paper. We derive the cell size at the onset of the cell cycle in Sect. II, and the stationary cell size of the model in Sect. III. They are expressed by sums of lognormal variables, and the corresponding cell-size distributions are not exactly lognormal. We propose a quantity which evaluates how far the cell size is different from the lognormal behavior. We numerically show that the deviation from the lognormality depends on the product variable of the growth rate and cell cycle, and derive its scaling property. From these results, the cell-size distribution of *B. subtilis* is suggested to be only a lognormal-like distribution, but it can be approximated well by a lognormal distribution owing to the parameter values of the growth rate and cell cycle which give good lognormal approximation.

II. ANALYSIS 1: CELL SIZE JUST AFTER THE CELL DIVISION

The aim of this study is to obtain the stationary cell-size distribution of the model, but it is complicated to derive it firsthand. At each moment, there exist cells soon after the division, some time after the division, and just before the next division. We need to consider the variation of the time passed from the previous division. Before studying this cell-size distribution, we start with the cell-size distribution limited to the cells just divided, which is a simpler problem.

We focus on the cell size at the onset of the cell cycle, and introduce a random variable X'_n as the initial cell size

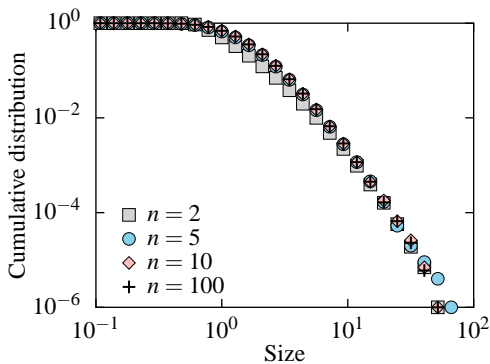


FIG. 2: Cumulative distributions of X'_n for $n = 2$ (squares), 5 (circles), 10 (diamonds), and 100 (crosses). Each of them is made by 10^6 independent samples, where $\mu_L = 0$ and $\sigma_L = 1$.

at the n th cell cycle. By setting V_n as the n th growth rate and T_n as the n th cell cycle, the growth increment during the n th cycle is expressed as $V_n T_n$. The cell size at the end of this cycle is $X'_n + V_n T_n$. This length is split in half in the cell division, so X'_{n+1} is given by

$$X'_{n+1} = \frac{1}{2}X'_n + \frac{1}{2}V_n T_n. \quad (2)$$

We easily obtain its solution

$$X'_n = \frac{1}{2^{n-1}} + \sum_{k=1}^{n-1} \frac{V_k T_k}{2^{n-k}} \quad (3)$$

by applying Eq. (2) recursively and using the initial condition $X'_1 = 1$. Note that the effect of the initial length X'_1 vanishes exponentially as n increases.

Random variables V_k and T_k always appear in the form of the product $V_k T_k$ throughout this paper, and we set a new random variable $L_k := V_k T_k$. In light of the experiment, V_k and T_k in the model are lognormal variables. The product L_k is therefore a lognormal variable, because the product of two independent lognormal variables again follows a lognormal distribution [3]. We put $\ln \mathcal{N}(\mu_L, \sigma_L^2)$ for the distribution of L_k , and investigate properties of X'_n against μ_L and σ_L . The model assumes that V_k 's and T_k 's are independent, and hence L_k 's are independently and identically distributed. Hence, X'_n is given by the sum of independent lognormal variables.

By using the average and variance of L_k 's

$$E[L_1] = E[L_2] = \dots = e^{\mu_L + \sigma_L^2/2}, \quad (4a)$$

$$V[L_1] = V[L_2] = \dots = e^{2\mu_L + \sigma_L^2}(e^{\sigma_L^2} - 1), \quad (4b)$$

the average and variance of X'_n are respectively calcu-

lated as

$$\begin{aligned} E[X'_n] &= \frac{1}{2^{n-1}} + \sum_{k=1}^{n-1} \frac{E[L_k]}{2^{n-k}} \\ &= e^{\mu_L + \sigma_L^2/2} - \frac{e^{\mu_L + \sigma_L^2/2} - 1}{2^{n-1}}, \\ V[X'_n] &= \sum_{k=1}^{n-1} \frac{V[L_k]}{4^{n-k}} \\ &= \frac{e^{2\mu_L + \sigma_L^2}(e^{\sigma_L^2} - 1)}{3} - \frac{e^{2\mu_L + \sigma_L^2}(e^{\sigma_L^2} - 1)}{3 \cdot 4^{n-1}}. \end{aligned}$$

They converge exponentially as $n \rightarrow \infty$. As shown in Fig. 2, the distribution of X'_n also rapidly becomes stationary; the distributions for $n = 10$ and 100 appear to be almost unchanged. In the numerical calculations below, therefore, we use the distribution for $n = 10$ as a substitute for the stationary distribution.

The variable X'_n is given by the weighted sum of independent and identical lognormal variables L_k 's. A sum of lognormal variables does not follow a lognormal distribution exactly. (Compare that a sum of normal variables again follows a normal distribution.) However, such a sum variable can be approximated by a single lognormal distribution. Among many techniques to approximate a lognormal sum by a single lognormal distribution [27–29], the simplest and fastest method is the Fenton-Wilkinson (FW) approximation [25], in which the lognormal parameters are estimated by matching the first and second moments. When sample values $\{x_1, \dots, x_N\}$ of X'_n are given, the best lognormal distribution $\ln \mathcal{N}(\hat{\mu}, \hat{\sigma}^2)$ in the FW sense is determined by

$$\begin{aligned} e^{\hat{\mu} + \hat{\sigma}^2/2} &= \frac{x_1 + \dots + x_N}{N} =: m_1, \\ e^{2(\hat{\mu} + \hat{\sigma}^2)} &= \frac{x_1^2 + \dots + x_N^2}{N} =: m_2. \end{aligned}$$

The left-hand sides are the first and second moments of $\ln \mathcal{N}(\hat{\mu}, \hat{\sigma}^2)$. The estimates $\hat{\mu}$ and $\hat{\sigma}$ are explicitly written as

$$\hat{\mu} = 2 \ln m_1 - \frac{1}{2} \ln m_2, \quad \hat{\sigma}^2 = \ln m_2 - 2 \ln m_1. \quad (5)$$

In addition to its simplicity, the FW method is known to approximate well in tail of the cumulative distribution [26]. Since we mainly focus on the cumulative distribution, the FW method is suitable for this study.

We numerically investigated whether X'_n is approximated by a lognormal distribution. For each μ_L and σ_L , we generated independent samples $\{x_1, \dots, x_N\}$ of X'_n by using Eq. (3), and estimated $\hat{\mu}$ and $\hat{\sigma}$ by the FW approximation (5). To evaluate the validity of the lognormal approximation, we calculated the difference between the estimated lognormal distribution $F_{\hat{\mu}, \hat{\sigma}}$ and the empirical cumulative distribution of $\{x_1, \dots, x_N\}$ defined by

$$G(x) = \frac{\text{number of elements} \geq x}{N}.$$

We define the difference as

$$D = \left[\int_0^\infty (F_{\hat{\mu}, \hat{\sigma}}(x) - G(x))^2 dx \right]^{1/2}.$$

When the set of samples $\{x_1, \dots, x_N\}$ fits well to the lognormal distribution, D becomes small. We use cumulative distributions $F_{\hat{\mu}, \hat{\sigma}}$ and G in the definition of D , because we are primarily interested in whether the tail of $G(x)$ exhibits lognormal decay. For simplicity, we assume that $\{x_1, \dots, x_N\}$ is arranged in descending order ($x_1 \geq \dots \geq x_N$), which yields $G(x_i) = i/N$. We replace the integral of D with a Riemann sum as

$$\begin{aligned} \Delta &= \left[\sum_{i=1}^{N-1} (F_{\hat{\mu}, \hat{\sigma}}(x_i) - G(x_i))^2 (x_i - x_{i+1}) \right]^{1/2} \\ &= \left[\sum_{i=1}^{N-1} \left(F_{\hat{\mu}, \hat{\sigma}}(x_i) - \frac{i}{N} \right)^2 (x_i - x_{i+1}) \right]^{1/2}. \end{aligned}$$

This is a discrete form of D .

In Fig. 3, we illustrate the numerical result of how close the stationary distribution of X'_n is to the lognormal distribution. We generated 10^4 independent samples of X'_{10} by Eq. (3) (recall that the distribution of X'_n appears to become stationary even at $n = 10$), estimated $\hat{\mu}$ and $\hat{\sigma}$ by the FW method, and computed Δ . Figure 3a is a contour plot of Δ in the (μ_L, σ_L) plane. The distribution of X'_{10} deviates from lognormal distribution (i.e., Δ becomes large) as σ_L and μ_L increase. Figures 3b and c show profile curves at fixed σ_L ($\sigma_L = 0.2, 0.5$, and 1) and μ_L ($\mu_L = 0, 2$, and 5), respectively.

The dependence of Δ on μ_L (Fig. 3b) can be explained briefly as follows. If we multiply $\{x_1, \dots, x_N\}$ by a factor e^α to have $\{e^\alpha x_1, \dots, e^\alpha x_N\}$, the lognormal estimates become $\hat{\mu} + \alpha$ and $\hat{\sigma}^2$. Since the scaling relation $F_{\hat{\mu}+\alpha, \hat{\sigma}}(e^\alpha x_i) = F_{\hat{\mu}, \hat{\sigma}}(x_i)$ holds from Eq. (1), Δ of the sample $\{e^\alpha x_i\}$ is expressed as

$$\begin{aligned} \Delta(\{e^\alpha x_i\}) &= \left[\sum_{i=1}^N \left(F_{\hat{\mu}+\alpha, \hat{\sigma}}(e^\alpha x_i) - \frac{i}{N} \right)^2 (e^\alpha x_{i+1} - e^\alpha x_i) \right]^{1/2} \\ &= \left[e^\alpha \sum_{i=1}^N \left(F_{\hat{\mu}, \hat{\sigma}}(x_i) - \frac{i}{N} \right)^2 (x_{i+1} - x_i) \right]^{1/2} \\ &= e^{\alpha/2} \Delta(\{x_i\}). \end{aligned}$$

Hence, multiplying $\{x_i\}$ by e^α causes the factor $\exp(\alpha/2)$ to Δ . Meanwhile, multiplying $\{x_i\}$ by e^α corresponds to replacing $L_k (= V_k T_k)$ in Eq. (3) with $e^\alpha L_k$. Since $e^\alpha L_k$ follows $\ln \mathcal{N}(\mu_L + \alpha, \sigma_L^2)$, using $e^\alpha L_k$ instead of L_k implies adding α to μ_L . Finally, $\Delta \propto \exp(\mu_L/2)$ is derived. We numerically confirmed this relation (see Fig. 4). Figure 4a shows that the graphs in Fig. 3b grow exponentially. Thus, the three graphs in Fig. 3c are collapsed into a single curve by using the scaled value $\Delta / \exp(\mu_L/2)$, as shown in Fig. 4b. In short, the increase of Δ against μ_L is simply due to the scaling effect of Δ .

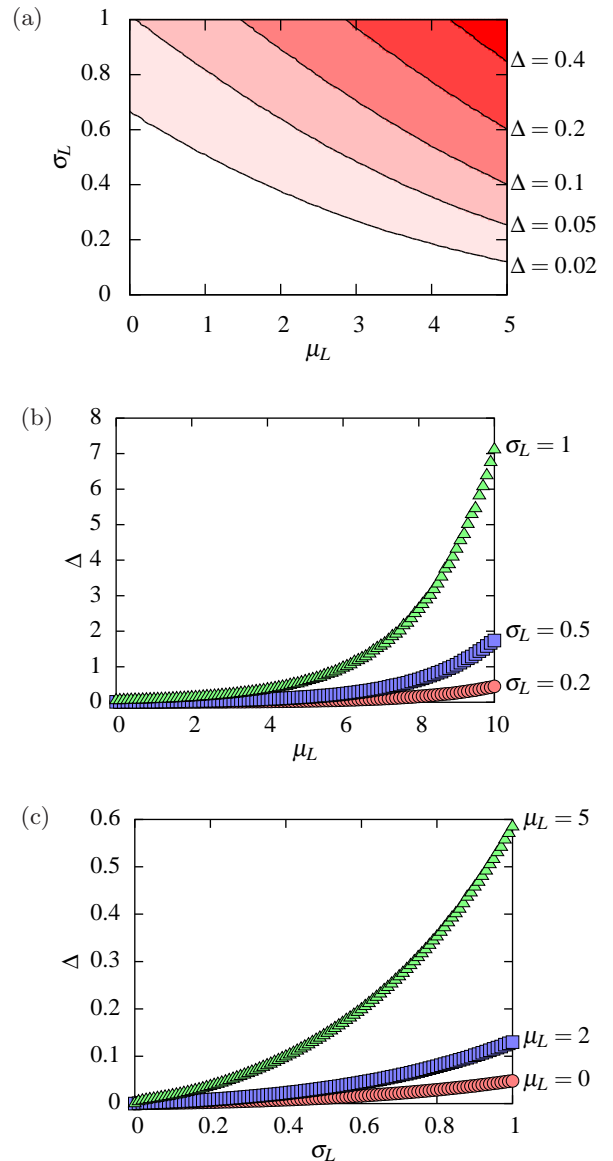


FIG. 3: Quality of the FW approximation to the distribution of X'_n ($n = 10$). (a) Contour plot of Δ in the (μ_L, σ_L) plane. Contours of $\Delta = 0.02, 0.05, 0.1, 0.2$, and 0.4 are shown by the solid curves. (b) Graphs of Δ vs. μ_L at $\sigma_L = 0.2, 0.5$, and 1 . (c) Graphs of Δ vs. σ_L at $\mu_L = 0, 2$, and 5 .

III. ANALYSIS 2: STATIONARY CELL-SIZE DISTRIBUTION IN THE MODEL

In this section, we investigate the cell-size distribution after a long time in the model, which also corresponds to the experimental cell-size distribution. Note that this distribution involves all cells, not only cells just after the division. Thus, the distribution is different from X'_n stated in the previous section.

After a long time that the cells go through cell divisions many times, the cell size just after the division is written

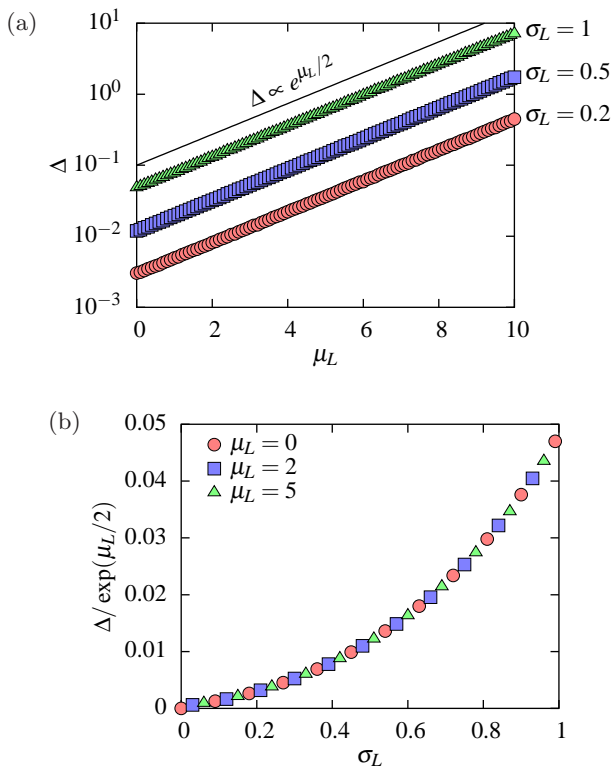


FIG. 4: Scaling property of Δ . (a) Δ grows exponentially with μ_L . The relation $\Delta \propto \exp(\mu_L/2)$ is shown by the solid line. (b) The graphs in Fig. 3b collapse to a single curve by scaling Δ by a factor $\exp(\mu_L/2)$. Different points are alternately aligned in order to avoid overlapping.

as

$$X'_\infty = \sum_{k=1}^{\infty} \frac{L_k}{2^k}. \quad (6)$$

This expression is obtained by taking the limit $n \rightarrow \infty$ in Eq. (3). In this stationary state, the cell size just before the division is given by $L_0 + X'_\infty$, where L_0 is a lognormal variable with $\ln \mathcal{N}(\mu_L, \sigma_L^2)$. At an arbitrary time, a randomly chosen cell takes a random size between X'_∞ and $L_0 + X'_\infty$ uniformly. The size of a cell randomly chosen at an arbitrary time is therefore written as

$$X = rL_0 + \sum_{k=1}^{\infty} \frac{L_k}{2^k}, \quad (7)$$

where r is a uniform random number on the unit interval $[0, 1]$, and L_0, L_1, \dots are independently and identically distributed with the lognormal distribution $\ln \mathcal{N}(\mu_L, \sigma_L^2)$. The first term rL_0 on the right-hand side represents the fluctuation of the time passed from the previous cell division. Note that $r = 0$ and $r = 1$ respectively correspond to the cell sizes just after the division and just before the division.

We numerically checked that Eq. (7) gives a proper cell-size distribution corresponding to the model (see

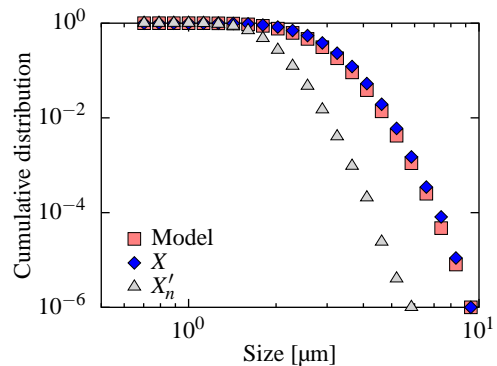


FIG. 5: Cell-size distributions of direct simulation of the model (squares), X (diamonds) and X'_∞ (triangles). The distribution of X is close to that of direct simulation, but the distribution of X'_∞ is not.

Fig. 5). The square plots named “model” are the cell-size distribution obtained by directly simulating the time evolution of cells along the procedure of the model (as in Fig. 1). The cell cycles and growth rates were drawn from the lognormal distributions $\ln \mathcal{N}(3.1, 0.20^2)$ and $\ln \mathcal{N}(-2.6, 0.30^2)$, respectively. We computed the cell size distribution when the total number of cells became 10^6 . The diamonds are the distribution of X made by 10^6 samples, in which we replaced the infinite sum in Eq. (7) with the first ten terms. These two graphs are very close to each other, which indicates that Eq. (7) is a valid expression. The distribution of X'_n ($n = 10$) is shown as the triangles, but is obviously away from the others.

It is not clear whether the distribution of X is approximated by a single lognormal distribution. We show in Fig. 6 the validity of lognormal approximation of X by the FW method. As with Fig. 3, we calculated Δ by using 10^4 samples of X , in which the infinite sum in Eq. (7) was replaced with the first ten terms. Figure 6a is a contour plot of Δ in the (μ_L, σ_L) plane. The shape of contour lines is more intricate than Fig. 3a. Figures 6b and c respectively illustrate profile curves at fixed σ_L ($\sigma_L = 0.2, 0.5$, and 1) and μ_L ($\mu_L = 0, 2$, and 5). The curves in Fig. 6c are not monotonic, and they take the minimum values at $\sigma_L = 0.43$ – 0.44 in common. That is, the distribution of X is greatly inconsistent with a lognormal distribution when σ_L is too small or too large. By using the scaled value $\Delta / \exp(\mu_L/2)$, the curves in Fig. 6c are collapsed into a single curve (see Fig. 6d).

In Fig. 7, the distributions of X with $\mu_L = 0$ and $\sigma_L = 0.2$ (lower triangles), 0.4 (circles), and 0.8 (upper triangles) are presented. The lognormal distributions by the FW approximation are shown by the solid curves. The distribution of $\sigma_L = 0.4$ (near the bottom of the curve in Fig. 6d) totally fits the lognormal distribution. In contrast, the distribution of $\sigma_L = 0.2$ decays faster than the lognormal, and that of $\sigma_L = 0.8$ decays slower than the lognormal.

In the actual growth of *B. subtilis*, the growth rate V_k

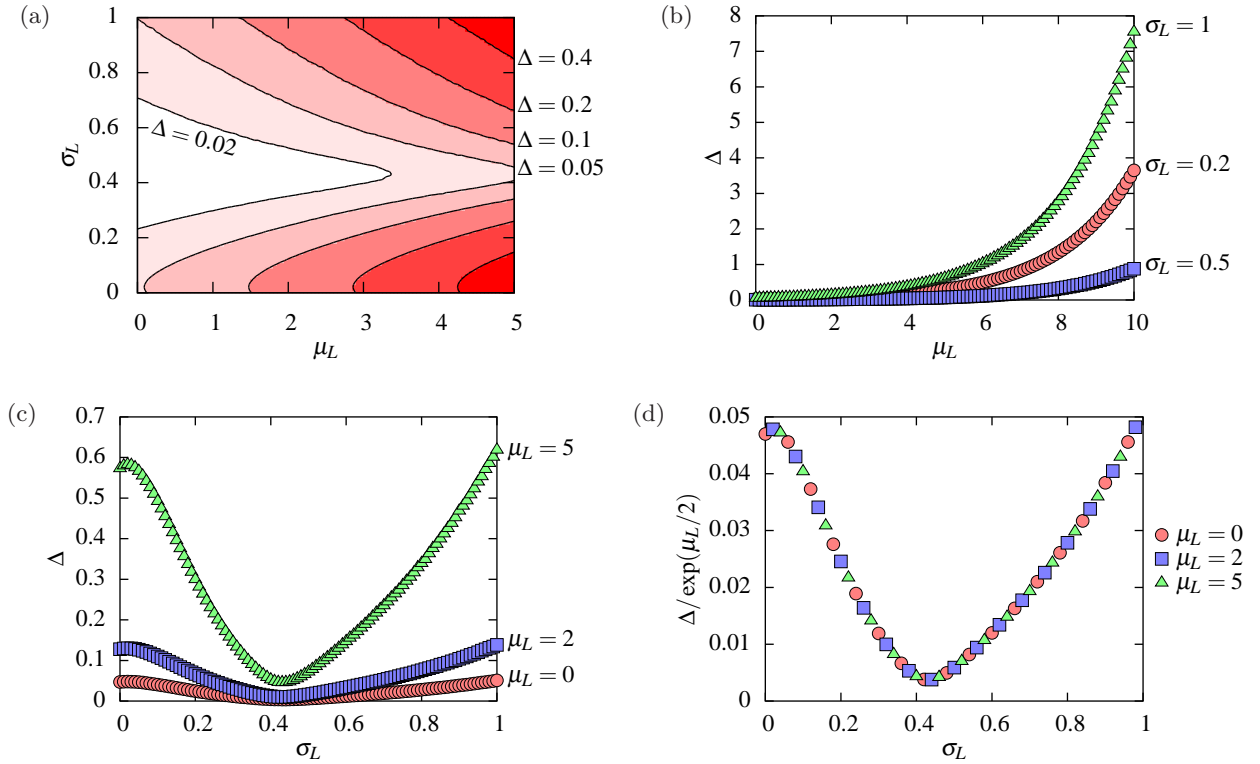


FIG. 6: Properties of Δ for the distribution of X . (a) Contour plot of Δ in the (μ_L, σ_L) plane. (b), (c) Profile curves at fixed σ_L ($\sigma_L = 0.2, 0.5$, and 1) and μ_L ($\mu_L = 0, 2$, and 5), respectively. (d) The curves in (c) overlap to each other by using the scaled value $\Delta / \exp(\mu_L/2)$. As with Fig. 4b, different points are aligned alternately.

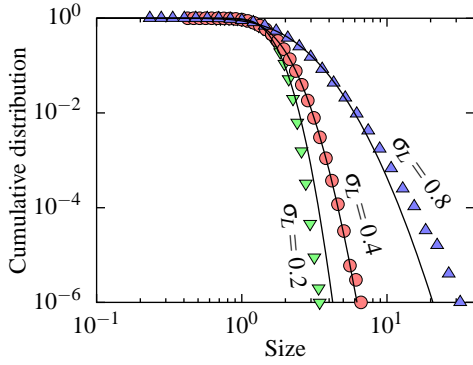


FIG. 7: Comparison of distributions of X with $\mu_L = 0$ and $\sigma_L = 0.2$ (lower triangles), 0.4 (circles), and 0.8 (upper triangles). The solid curves are the lognormal approximation results by using the FW method.

and cell cycle T_k respectively obey $\ln \mathcal{N}(\ln 22, 0.20^2)$ and $\ln \mathcal{N}(\ln 0.078, 0.30^2)$. The distribution of their product $L_k = V_k T_k$ is then given by

$$\ln \mathcal{N}(\ln 22 + \ln 0.078, 0.20^2 + 0.30^2) = \ln \mathcal{N}(0.54, 0.36^2).$$

We note that $\sigma_L = 0.36$ is near the bottom of the curve in Fig. 6d at which Δ becomes small. This is a theoretical reason why the actual cell-size distribution of *B. subtilis* agrees very well with a lognormal distribution.

The average of X is easily calculated as

$$E[X] = E[r]E[L_0] + \sum_{k=1}^{\infty} \frac{E[L_k]}{2^k} = \frac{3}{2} e^{\mu_L + \sigma_L^2/2},$$

where we used Eq. (4a) and $E[r] = 1/2$ (average of the uniform random number on $[0, 1]$). The variance of X is calculated as

$$V[X] = V[rL_0] + \sum_{k=1}^{\infty} \frac{V[L_k]}{4^k} = \frac{2}{3} e^{2\mu_L + 2\sigma_L^2} - \frac{7}{12} e^{2\mu_L + \sigma_L^2},$$

where we used Eq. (4b) and the formula[30]

$$V[rL_0] = V[r]V[L_0] + E[r]^2V[L_0] + V[r]E[L_0]^2$$

for the variance of the product, with $V[r] = 1/12$. The square average of X is then given by

$$E[X^2] = V[X] + E[X]^2 = \frac{2}{3} e^{2\mu_L + 2\sigma_L^2} + \frac{5}{3} e^{2\mu_L + \sigma_L^2}.$$

The parameter $\hat{\mu}$ of the FW approximation is

$$\hat{\mu} = 2 \ln E[X] - \frac{1}{2} \ln E[X^2],$$

where we substitute $E[X]$ and $E[X^2]$ for m_1 and m_2 in Eq. (5), respectively. We then obtain the median of X

$$e^{\hat{\mu}} = \frac{E[X]^2}{E[X^2]^{1/2}} = \frac{9\sqrt{3}}{4} \frac{e^{\mu_L}}{(2 + 5e^{-\sigma_L^2})^{1/2}}.$$

With this result, we can compute the median of the stationary cell size X from two parameters μ_L and σ_L . By using the values $\mu_L = 0.54$ and $\sigma_L = 0.36$ from the experiment, we have

$$e^{\hat{\mu}} \approx 2.65 \mu\text{m}.$$

This estimate correctly gives the experimental median $2.7 \mu\text{m}$ of the cell size.

IV. DISCUSSION

In this paper, we have solved the phenomenological stochastic model for bacterial growth, and have shown that the stationary cell size (7) is expressed by using lognormal variables and a uniform variable. This result suggests that the cell size of *B. subtilis* does not follow a genuine lognormal distribution but a lognormal-like distribution. The parameter σ_L is important for the quality of the lognormal approximation. This study has elucidated that the value $\sigma_L = 0.36$ for the actual bacterial growth, which is near the bottom of Fig. 6d ($\sigma_L \approx 0.43$), is the reason why the experimental cell-size distribution can be approximated well by a lognormal distribution. The value of σ_L can be varied by changing external conditions or using other bacterial species such as *Escherichia coli*[31] and *Proteus mirabilis*[32]. We expect that the model and analysis in this study is quantitatively inspected by estimating σ_L and Δ from experiments under these conditions.

We make a further comparison between our result and a numerical result of Wakita *et al.*[22] in which the cell cycle T_k and growth rate V_k are varied separately. Here we set $\ln\mathcal{N}(\mu_T, \sigma_T^2)$ and $\ln\mathcal{N}(\mu_V, \sigma_V^2)$ for the distributions of T_k and V_k , respectively. Wakita *et al.*[22] have investigated the lognormality of the stationary cell-size distribution of the model in the (σ_T, σ_V) plane, instead of σ_L , with fixed medians $\exp(\mu_T) = 20$ min and $\exp(\mu_V) = 0.1 \mu\text{m}/\text{min}$. This result is shown by the circles (the lognormal approximation is valid) and upper and lower triangles (the lognormal approximation is not good) in Fig. 8. The size distribution deviates from the lognormal for small σ_T and σ_V or for large σ_T and σ_V . In this figure, the contours of $\Delta = 0.01, 0.02$, and 0.04 are also shown by the solid curves. The relation $\sigma_L^2 = \sigma_T^2 + \sigma_V^2$ is obtained from $L_k = V_k T_k$, and hence, the curve of $\sigma_L = \text{const}$ forms an arc centered at the origin in the (σ_T, σ_V) plane. The value of Δ depends on σ_L and not on σ_T and σ_V , so the contours of Δ are concentric circles. In contrast, the boundary between circles and lower triangles seems to be a straight line. We deduce that this difference arises because the judgment of circle or triangle has relied on human eyes. Nevertheless, we consider our result to be consistent with the previous study as a whole. In fact, the region of $\Delta < 0.01$ contains only circle points, and that of $\Delta > 0.02$ contains lower triangle points. Moreover, circles and lower triangles exist in a narrow range $0.01 < \Delta < 0.02$.

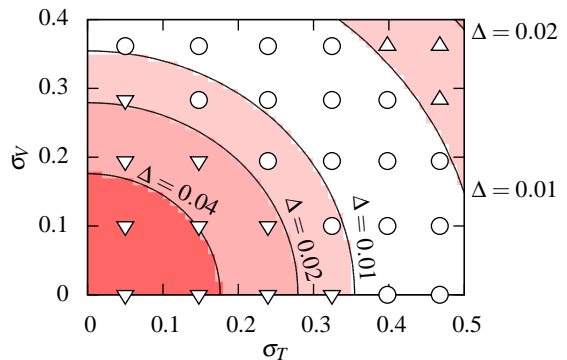


FIG. 8: Quality of the lognormality of the stationary cell-size distribution in the (σ_T, σ_V) plane. The circles (showing that the lognormal approximation is valid) and upper and lower triangles (lognormal approximation is invalid) are results of Wakita *et al.*[22]. Contours of $\Delta = 0.01, 0.02$, and 0.04 are shown by solid curves.

The model assumes the lognormality of the growth rate V_k and cell cycle T_k . (Theoretically, the lognormality of their product $L_k = V_k T_k$ is essential in our analysis.) As a matter of fact, however, it is unclear why they follow lognormal distributions. At the same time, we cannot exclude the possibility that they actually follow lognormal-like distributions. Stochastic properties of V_k and T_k may involve dynamics inside a cell, and this is a problem for future research. Increasing experimental data can also help to investigate V_k and T_k more minutely.

The difference Δ between a cell-size distribution and its FW approximate becomes large when σ_L increases both in Figs. 3a and 6a. This behavior has been found also in a finite sum of lognormal variables[27]. For small σ_L , on the other hand, Δ for X (Fig. 6a) is greatly different from that for X'_∞ (Fig. 3a). Let us consider a limiting case $\sigma_L = 0$; that is, the random variable L_k is constant [$L_k \equiv \exp(\mu_L)$]. X'_∞ in Eq. (6) is also constant [$X'_\infty \equiv \exp(\mu_L)$], and X'_∞ is distributed lognormally with $\ln\mathcal{N}(\mu_L, 0)$. Thus, $\Delta = 0$ for X'_∞ . (We can observe $\Delta \rightarrow 0$ as $\sigma_L \rightarrow 0$ in Fig. 3c.) On the other hand, the random variable rL_0 in Eq. (7) is uniformly distributed in the interval $[0, \exp(\mu_L)]$, and $X (= rL_0 + X'_\infty)$ is uniformly distributed on $[\exp(\mu_L), 2\exp(\mu_L)]$. The uniform distribution is different from a lognormal distribution, so Δ for X does not become zero as $\sigma \rightarrow 0$. Thus, the property of Δ for small σ_L is influenced by the term “ rL_0 ” in Eq. (7). We conjecture that the balance of the increase of Δ for large σ_L and the existence of the term rL_0 forms the minimum point of Fig. 6d, but we have not yet carried out a detailed analysis, especially why the minimum is at $\sigma_L \approx 0.43$.

In order to comprehend complex systems, we usually describe a phenomenon broadly by neglecting its details at first, and gradually increase accuracy. In this paper, we have investigated how much the actual distribution is deviated from the approximate lognormal distribution, which is the deepening of the result that the cell-size

distribution is close to the lognormal distribution. Lognormal behavior has been reported in many systems in a first approximation, and we hope that our analysis helps to develop further research of such systems.

Acknowledgments

The authors are very grateful to H. R. Brand for the fruitful discussion of the manuscript. This work was

supported by a Grant-in-Aid for Young Scientists (B) (25870743) from the Japan Society for the Promotion of Science (KY), and a Chuo University Grant for Special Research and a Grant-in-Aid for Exploratory Research (15K13537) from JSPS (JW).

-
- [1] M. E. J. Newman, *Contemp. Phys.* 46, 323 (2005).
 [2] M. Buchanan, *Ubiquity: Why Catastrophes Happen* (Three Rivers Press, New York, 2000).
 [3] E. L. Crow and K. Shimizu, *Lognormal Distributions* (Dekker, New York, 1988).
 [4] N. Kobayashi, H. Kuninaka, J. Wakita, and M. Matsushita, *J. Phys. Soc. Jpn.* 80, 072001 (2011).
 [5] E. Limpert, W. A. Stahel, and M. Abbt, *BioScience* 51, 341 (2001).
 [6] H. Katsuragi, D. Sugino, and H. Honjo, *Phys. Rev. E* 70, 065103(R) (2004).
 [7] M. Bittelli, G. S. Campbell, and M. Flury, *Soil Sci. Soc. America J.* 63, 782 (1998).
 [8] P. Uttley, I. M. McHardy, and S. Vaughan, *Mon. Not. R. Astron. Soc.* 359, 345 (2005).
 [9] C. Furusawa, T. Suzuki, A. Kashiwagi, T. Yomo, and K. Kaneko, *Biophys. J.* 1, 25 (2005).
 [10] Y. Sasaki, H. Kuninaka, and M. Matsushita, *J. Phys. Soc. Jpn.* 76, 074801 (2007).
 [11] S. Redner, *Phys. Today* 58 [6], 49 (2005).
 [12] S. Fortunato and C. Castellano, *Phys. Rev. Lett.* 99, 138701 (2007).
 [13] M. Abramowitz and I. A. Stegun, *Handbook of Mathematical Functions* (Dover, New York, 1965).
 [14] D. Sornette, *Critical Phenomena in Natural Sciences*, 2nd ed. (Springer, Berlin, 2006).
 [15] M. Mitzenmacher, *Internet Math.* 1, 226 (2004).
 [16] Y. Malevergne, V. Pisarenko, and D. Sornette, *Phys. Rev. E* 83, 036111 (2011).
 [17] H. Kuninaka, Y. Mitsuhashi, and M. Matsushita, *J. Phys. Soc. Jpn.* 78, 125001 (2009).
 [18] M. P. H. Stumpf and P. J. Ingram, *Europhys. Lett.* 71, 152 (2005).
 [19] H. Takayasu, A. Sato, and M. Takayasu, *Phys. Rev. Lett.* 79, 966 (1999).
 [20] S. C. Manrubia and D. H. Zanette, *Phys. Rev. E* 59, 4945 (1999).
 [21] K. Yamamoto and Y. Yamazaki, *Phys. Rev. E* 85, 011145 (2012).
 [22] J. Wakita, H. Kuninaka, T. Matsuyama, and M. Matsushita, *J. Phys. Soc. Jpn.* 79, 094002 (2010).
 [23] M. Matsushita, F. Hiramatsu, N. Kobayashi, T. Ozawa, Y. Yamazaki, and T. Matsuyama, *Biofilms* 1, 305 (2004).
 [24] T. Vicsek, *Fluctuations and Scaling in Biology* (Oxford University Press, New York, 2001).
 [25] L. F. Fenton, *IRE Trans. Commun. Syst.* 8, 57 (1960).
 [26] A. A. Abu-Dayya and N. C. Beaulieu, *IEEE Trans. Vehicular Tech.* 43, 163 (1994).
 [27] S. C. Schwartz and Y. S. Yeh, *Bell System Technical Journal* 61, 1441 (1982).
 [28] C.-L. Ho, *IEEE Trans. Vehicular Technology* 44, 756 (1995).
 [29] N. B. Mehta, J. Wu, A. F. Molisch, and J. Zhang, *IEEE Trans. Wireless Communications* 6, 2690 (2007).
 [30] L. A. Goodman, *J. American Stat. Association* 55, 708 (1960).
 [31] M. Fujihara, J. Wakita, D. Kondoh, M. Matsushita, and R. Harasawa, *African J. Microbiol. Res.* 7, 1780 (2013).
 [32] T. Matsuyama, Y. Takagi, Y. Nakagawa, H. Itoh, J. Wakita, and M. Matsushita, *J. Bacteriol.* 182, 385 (2000).